Original Article

Institution of MECHANICAL ENGINEERS
Journal of MECHANICAL ENGINEERING SCIENCE

Bending and free vibration analyses of functionally graded material nanoplates via a novel nonlocal single variable shear deformation plate theory

Proc IMechE Part C:
J Mechanical Engineering Science
0(0) 1–13

DOI: 10.1177/0954406220964522
journals.sagepub.com/home/pic
SAGE

Le Kha Hoa[1,2], Pham Van Vinh[3], Nguyen Dinh Duc[4,5,6], Nguyen Thoi Trung[1,2], Le Truong Son[3] and Do Van Thom[3]

Abstract

A novel nonlocal shear deformation theory is established to investigate functionally graded nanoplates. The significant benefit of this theory is that it consists of only one unknown variable in its displacement formula and governing differential equation, but it can take into account both the quadratic distribution of the shear strains and stresses through the plate thickness as well as the small-scale effects on nanostructures. The numerical solutions of simply supported rectangular functionally graded material nanoplates are carried out by applying the Navier procedure. To indicate the accuracy and convergence of this theory, the present solutions have been compared with other published results. Furthermore, a deep parameter study is also carried out to exhibit the influence of some parameters on the response of the functionally graded material nanoplates.

Keywords

Functionally graded material nanoplates, Navier solution, nonlocal theory, single variable shear deformation, bending, vibration

Date received: 16 April 2020; accepted: 11 September 2020

Introduction

In the last decades of the twentieth century, functionally graded materials (FGMs) have been become the most innovative composite materials and applied in many fields of engineering.[1–5] Because of their exotic properties, the application and investigation of FGM beams, plates and shells are increasing rapidly. Therefore, enormous beam, plate and shell theories were established and applied to scrutinize FGM structures, especially FGM plates. First of all, classical plate theory (CPT) has been applied to study beams and plates by many scientists such as Liessa,[6] Mohammadi[7] and so on. However, the CPT neglects the shear strains and stresses, so it is compatible to research thin plates only. Using this theory to analyze thick plate may result in absolutely erroneous solutions and consequently wrong designs. To deal with this shortcoming of CPT, Mindlin[8] developed a new plate theory which was so-called Mindlin plate theory. The benefit of this theory is that it is compatible to analyze thin to moderately thick plates, because it takes into account the influence of the shear strains and stresses. After that, the first-order shear deformation plate theory (FSDT) was developed and applied to study thin to thick plates. Some valuable works using FSDT can be seen in Hosseini-Hashemiand et al.,[9,10] Nguyen et al.[11] Continuously, many modified FSDTs have been established to reduce the number of unknown variables of the displacement formula. The information about these theories can be found in some works of

[1]Division of Computational Mathematics and Engineering, Institute for Computational Science, Ton Duc Thang University, Ho Chi Minh City, Vietnam
[2]Faculty of Civil Engineering, Ton Duc Thang University, Ho Chi Minh City, Viet Nam
[3]Department of Solid Mechanics, Le Quy Don Technical University, Hanoi City, Vietnam
[4]Advanced Materials and Structures Laboratory, VNU Hanoi, University of Engineering and Technology, Hanoi, Vietnam
[5]Infrastructure Engineering Program, VNU Hanoi, Vietnam-Japan University, Hanoi, Vietnam
[6]National Research Laboratory, Department of Civil and Environmental Engineering, Sejong University, Seoul, Korea

Corresponding authors:
Do Van Thom, Department of Solid Mechanics, Le Quy Don Technical University, Hanoi City, Vietnam.
Email: thom.dovan.mta@gmail.com
Le Kha Hoa, Institute for Computational Science, Ton Duc Thang University, Ho Chi Minh City, Vietnam.
Email: lekhahoa@tdtu.edu.vn

Shimpi et al.,[12] Thai et al.,[13] Nam et al.,[14] Nguyen et al.[15] The FSDT and its variants have been employed to investigate isotropic and orthotropic plates. The numerical results of these works were useful in many fields of engineering and industry. However, the shear strains and stresses of these theories do not equal to zero at two surfaces of the plates. On the other hand, FSDT and its variants need a shear correction coefficient which is very difficult to determine the exact value. To overcome these inconveniences of FSDT and its variants, researchers have been established many higher-order shear deformations (HSDTs). Because of its advantages, a lot of different theories based on the idea of HSDT such as sinusoidal shear deformation, generalized shear deformation, four-variable refined plate theory, refined plate theory and their variants have been developed. These theories have been combined with other methods to scrutinize isotropic and FGM plates. The success of these theories is that the shear strains and stresses are parabolic distribution through the thickness, hence they do not need any shear correction factors. More information about these theories can be found in many papers which have been published by many researchers such as Javaheri et al.,[16] Ferreira et al.,[17] Talha et al.,[18] Mantari et al.,[19,20] Merazi and Hasaine Daouadji,[21–23] Mechab et al.[24] and Shimpi et al.[25,26] According to these works, the HSDTs are good accuracy and convergence and they can predict the behavior of the plates better than FSDT. Recently, many quasi-3D theories have been established to capture the stretching effect on the response of the plates. The formulae and applications of these theories can be found in the works of Zenkour,[27] Mantari et al.,[28,29] Adim et al.[30] and Thai et al.[31] On the other hand, quasi-3D theories have been combined with the Carrera unified formulation (CUF) to investigate a wide range of structures as shown in Neves et al.,[32,33] Carrera et al.[34] and so on. In these theories, the normal stress being the thickness direction does not neglect, so they can be applied to study thick and very thick plates.

Nowadays, FGMs are more and more applied to manufacture the micro/nanostructures such as biological building blocks, solar cells, artificial structures, micro/nano sensors, micro/nanoelectromechanical systems (MEMS and NEMS). The using of nanostructures is increasing in exponential principle, so they have attracted a lot of researchers' attention. The reason is that these structures can act in high-performance applications and exhibit delightful features. The computation of these structures is very different in comparison with the traditional structures. The small-scale effects on the behavior of these structures must be considered, therefore it is essential to develop different theories to evaluate these structures. Some noticeable theories have been established by many researchers, such as the modified couple stress theory (MCST),[35] the surface elasticity,[36–41] the strain gradient theory (SGT),[42–44] the micropolar theory[45] and the nonlocal elasticity theory (NET).[46–49] Among them, the NET which is first established by Erigen is widely applied to evaluate nanostructures, this theory is very simple and good accuracy. In the NET, the stress at any points in the solid body depends on the strains at all neighbor points. Based on NET, a large number of works have been published in the literature using different plate theories. The analysis of nanobeams and nano bars using NET and different shear deformation theories were investigated by Reddy et al.,[50,51] Zenkour et al.,[52–54] Thai et al.,[55] Şimşek et al.,[56] Eltaher et al.,[57] Nazemnezhad et al.[58] and Arefi et al.,[59] Sobhy and Zenkour[60–63] and so on. Whereas, the behavior of nanoplates are investigated by Aghababaei et al.,[64] Lu et al.,[65] Aksencer et al.,[66] Hashemi et al.,[67] Zenkour et al.,[68] Alzahrani et al.,[69] Sobhy[70–73] and Natarajan et al.[74] In these studies, the nonlocal elasticity based on many plate theories has been used to analyze the isotropic and orthotropic nanoplates such as FGM nanoplates subjected to the mechanical load or thermal-mechanical load. According to these investigations, the effects of small-scale on the behavior of nanostructures cannot be neglected. These numerical results are very useful to estimate and design the nanostructures, and it is necessary to take more studies in these fields.

This study aims to establish a novel nonlocal theory based on a single variable shear deformation plate theory (SDPT), and then it is employed to investigate FGM nanoplates. Some important problems are performed to demonstrate the accuracy of the proposed theory. The outline of this work is as follows: Section 1 gives general and basic information of FGMs, nanostructures as well as the investigations of these structures. Section 2 gives a brief review of FGM and section 3 introduces the nonlocal elasticity theory of Eringen. Next, section 4 presents step by step the development of novel NET based on single variable SDPT and section 5 shows the analytical solution based on Navier procedure. Continuously, section 6 reveals the verification study to show the accuracy and convergence of the proposed theory and section 7 indicates the numerical and graphical investigation of FGM nanoplates. Finally, section 8 summaries some important conclusions on the development of proposed theory as well as the numerical results of the current work.

Material properties of FGM

In this study, a rectangular FGM nanoplate as shown in Figure 1 is considered, the dimension of the plate is $a \times b \times h$. The material properties are calculated by

$$P(z) = P_m + (P_c - P_m)V_c \tag{1}$$

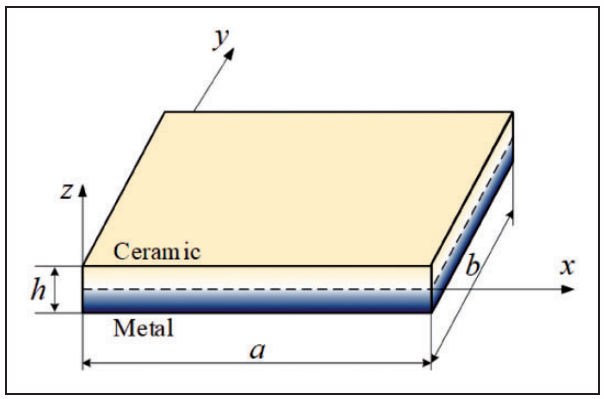

Figure 1. A model of FGM nanoplate.

$$V_c = \left(\frac{1}{2} + \frac{z}{h}\right)^p, \quad V_m = 1 - V_c \tag{2}$$

where P_c, P_m and V_c, V_m are respectively the Young's modulus or density and volume ratio of the ceramic and metal, p is the material parameter.

Nonlocal elasticity theory

In Eringen's nonlocal theory,[47] the stress at a point in a continuum body depends on the strains at all neighbor points. The differential form of this theory can be written as[48]

$$\Re\sigma = C\varepsilon \tag{3}$$

where $\Re = [1 - \kappa^2\nabla^2]$, $\kappa^2(nm^2) = (e_0a)^2$ is nonlocal coefficient and $\nabla^2 = \frac{\partial^2}{\partial x^2} + \frac{\partial^2}{\partial y^2}$. In which, the nonlocal coefficient should be $\kappa \leq 2$ for the most cases of nano-scale structures.[49]

Novel nonlocal single variable shear deformation plate theory

Assumption of novel nonlocal single variable shear deformation plate theory

The basic assumptions of novel nonlocal single variable SDPT are shown as follows

(i) Separating w into two parts, which are bending part w_b and shear part w_s.

$$w = w_b + w_s \tag{4}$$

(ii) The normal stress σ_z is very small, so it can be negligible.

(iii) The displacements u and v are separated into bending and shear parts as

$$\begin{aligned} u &= u_b + u_s \\ v &= v_b + v_s \end{aligned} \tag{5}$$

In which, u_b and v_b are similar to the displacements given by the CPT, which can be written as

$$u_b = -z\frac{\partial w_b}{\partial x}, \quad v_b = -z\frac{\partial w_b}{\partial y} \tag{6}$$

The shear parts u_s and v_s give rise to shear strain γ_{xz}, γ_{yz} and therefore to shear stresses τ_{xz}, τ_{yz}, and they distribute through the plate thickness. Subsequently, they can be obtained as

$$u_s = f(z)\frac{\partial w_s}{\partial x}, \quad v_s = f(z)\frac{\partial w_s}{\partial y} \tag{7}$$

The function $f(z)$ is given as the following formula

$$f(z) = \frac{z}{4} - \frac{5}{3}\frac{z^3}{h^2} \tag{8}$$

The formulas of moment resultants M_x, M_y, M_{xy} do not contain u_s and v_s.

(iv) It is assumed that only bending deflection produces the rotation of the plate cross-section, the inertia loading and distributed inertia moments can be obtained as

$$\bar{q} = -m_0\frac{\partial^2 w}{\partial t^2}, \quad m_x = -J_{0x}\frac{\partial^3 w_b}{\partial x \partial t^2}, \quad m_y = -J_{0y}\frac{\partial^3 w_b}{\partial y \partial t^2} \tag{9}$$

where

$$m_0 = \int_{-h/2}^{h/2} \rho(z)\,\mathrm{d}z, \quad J_{0x} = J_{0y} = J_0 = \int_{-h/2}^{h/2} \rho(z)z^2\,\mathrm{d}z \tag{10}$$

Expressions of displacement, force and moment resultants

Based on the previous section, the displacement field of the plate is

$$\begin{aligned} u &= -z\frac{\partial w_b}{\partial x} + f(z)\frac{\partial w_s}{\partial x} \\ v &= -z\frac{\partial w_b}{\partial y} + f(z)\frac{\partial w_s}{\partial y} \\ w &= w_b + w_s \end{aligned} \tag{11}$$

The formulas of the strain fields are

$$\begin{aligned} \varepsilon_x &= -z\frac{\partial^2 w_b}{\partial x^2} + f(z)\frac{\partial^2 w_s}{\partial x^2} \\ \varepsilon_y &= -z\frac{\partial^2 w_b}{\partial y^2} + f(z)\frac{\partial^2 w_s}{\partial y^2} \\ \gamma_{xy} &= -z\left(2\frac{\partial^2 w_b}{\partial x \partial y}\right) + f(z)\left(2\frac{\partial^2 w_s}{\partial x \partial y}\right) \\ \gamma_{xz} &= \frac{\partial w_s}{\partial x}r(z) \\ \gamma_{yz} &= \frac{\partial w_s}{\partial y}r(z) \end{aligned} \tag{12}$$

where $r(z) = 1 + f'(z)$.

By utilizing the NET and the Hooke's law, the nonlocal constitutive equations can be written as

$$\begin{aligned}\Re\sigma_x &= \frac{E(z)}{1-\nu(z)^2}\left[-z\frac{\partial^2 w_b}{\partial x^2}+f(z)\frac{\partial^2 w_s}{\partial x^2}\right.\\ &\quad\left.+\nu(z)\left(-z\frac{\partial^2 w_b}{\partial y^2}+f(z)\frac{\partial^2 w_s}{\partial y^2}\right)\right]\\ \Re\sigma_y &= \frac{E(z)}{1-\nu(z)^2}\left[-z\frac{\partial^2 w_b}{\partial y^2}+f(z)\frac{\partial^2 w_s}{\partial y^2}\right.\\ &\quad\left.+\nu(z)\left(-z\frac{\partial^2 w_b}{\partial x^2}+f(z)\frac{\partial^2 w_s}{\partial x^2}\right)\right]\\ \Re\tau_{xy} &= \frac{E(z)}{2(1+\nu(z))}\left(-2z\frac{\partial^2 w_b}{\partial x\partial y}+2f(z)\frac{\partial^2 w_s}{\partial x\partial y}\right)\end{aligned} \tag{13}$$

$$\begin{aligned}\Re\tau_{yz} &= \frac{r(z)E(z)}{2(1+\nu(z))}\frac{\partial w_s}{\partial y}\\ \Re\tau_{xz} &= \frac{r(z)E(z)}{2(1+\nu(z))}\frac{\partial w_s}{\partial x}\end{aligned} \tag{14}$$

Equations (13) and (14) can be rewritten in the following forms

$$\begin{aligned}\Re\sigma_x &= \frac{-zE(z)}{1-\nu(z)^2}\left(\frac{\partial^2 w_b}{\partial x^2}+\nu(z)\frac{\partial^2 w_b}{\partial y^2}\right)\\ &\quad+\frac{f(z)E(z)}{1-\nu^2}\left(\frac{\partial^2 w_s}{\partial x^2}+\nu(z)\frac{\partial^2 w_s}{\partial y^2}\right)\\ \Re\sigma_y &= \frac{-zE(z)}{1-\nu(z)^2}\left(\frac{\partial^2 w_b}{\partial y^2}+\nu(z)\frac{\partial^2 w_b}{\partial x^2}\right)\\ &\quad+\frac{f(z)E(z)}{1-\nu^2}\left(\frac{\partial^2 w_s}{\partial y^2}+\nu(z)\frac{\partial^2 w_s}{\partial x^2}\right)\\ \Re\tau_{xy} &= \frac{-zE(z)}{1-\nu(z)^2}(1-\nu(z))\frac{\partial^2 w_b}{\partial x\partial y}\\ &\quad+\frac{f(z)E(z)}{1-\nu(z)^2}(1-\nu(z))\frac{\partial^2 w_s}{\partial x\partial y}\end{aligned} \tag{15}$$

$$\begin{aligned}\Re\tau_{yz} &= \frac{r(z)E(z)}{2(1+\nu(z))}\frac{\partial w_s}{\partial y}\\ \Re\tau_{xz} &= \frac{r(z)E(z)}{2(1+\nu(z))}\frac{\partial w_s}{\partial x}\end{aligned} \tag{16}$$

The nonlocal moments and shear forces are obtained as

$$\Re\begin{Bmatrix}M_x\\M_y\\M_{xy}\end{Bmatrix} = \int_{-\frac{h}{2}}^{\frac{h}{2}} z\Re\begin{Bmatrix}\sigma_x\\\sigma_y\\\tau_{xy}\end{Bmatrix}\mathrm{d}z \tag{17}$$

$$\Re\begin{Bmatrix}Q_x\\Q_y\end{Bmatrix} = \int_{-\frac{h}{2}}^{\frac{h}{2}} \Re\begin{Bmatrix}\tau_{xz}\\\tau_{yz}\end{Bmatrix}\mathrm{d}z \tag{18}$$

Based on the assumption of the present theory, the nonlocal moments and shear forces can be taken as

$$\begin{aligned}\Re M_x &= \int_{-h/2}^{h/2}\frac{-z^2E(z)}{1-\nu(z)^2}\left[\frac{\partial^2 w_b}{\partial x^2}+\nu(z)\frac{\partial^2 w_b}{\partial y^2}\right]\mathrm{d}z\\ \Re M_y &= \int_{-h/2}^{h/2}\frac{-z^2E(z)}{1-\nu(z)^2}\left[\frac{\partial^2 w_b}{\partial y^2}+\nu(z)\frac{\partial^2 w_b}{\partial x^2}\right]\mathrm{d}z\\ \Re M_{xy} &= \int_{-h/2}^{h/2}\frac{-z^2E(z)}{(1-\nu(z)^2)}\left[(1-\nu(z))\frac{\partial^2 w_b}{\partial x\partial y}\right]\mathrm{d}z\end{aligned} \tag{19}$$

$$\begin{aligned}\Re Q_x &= \int_{-h/2}^{h/2}\frac{E(z)}{2(1+\nu(z))}r(z)\frac{\partial w_s}{\partial x}\,\mathrm{d}z\\ \Re Q_y &= \int_{-h/2}^{h/2}\frac{E(z)}{2(1+\nu(z))}r(z)\frac{\partial w_s}{\partial y}\,\mathrm{d}z\end{aligned} \tag{20}$$

After integrating equations (19) and (20) through the thickness, ones get

$$\begin{aligned}\Re M_x &= -D\frac{\partial^2 w_b}{\partial x^2}-D_1\frac{\partial^2 w_b}{\partial y^2}\\ \Re M_y &= -D\frac{\partial^2 w_b}{\partial y^2}-D_1\frac{\partial^2 w_b}{\partial x^2}\\ \Re M_{xy} &= -D\frac{\partial^2 w_b}{\partial x\partial y}+D_1\frac{\partial^2 w_b}{\partial x\partial y}\end{aligned} \tag{21}$$

$$\begin{aligned}\Re Q_x &= S\frac{\partial w_s}{\partial x}\\ \Re Q_y &= S\frac{\partial w_s}{\partial y}\end{aligned} \tag{22}$$

The coefficients D, D_1, S are calculated as

$$D = \int_{-h/2}^{h/2}\frac{z^2E(z)}{1-\nu(z)^2}\,\mathrm{d}z \tag{23}$$

$$D_1 = \int_{-h/2}^{h/2}\frac{z^2\nu(z)E(z)}{1-\nu(z)^2}\,\mathrm{d}z \tag{24}$$

$$S = \int_{-h/2}^{h/2}\frac{r(z)E(z)}{2(1+\nu(z))}\,\mathrm{d}z \tag{25}$$

The coefficients D, D_1 and S are the integration formulas respect to z and depend on the plate thickness, the material properties and the distributed shape function. In Shimpi's plate theory, the material is assumed that its properties do not change through the thickness, therefore D, D_1 and S are explicit expressions of the thickness.

The equilibrium equations of forces are

$$\begin{aligned}
&\frac{\partial}{\partial x}(\Re M_x)+\frac{\partial}{\partial y}(\Re M_{xy})-\Re Q_x=\Re m_x\\
&\frac{\partial}{\partial x}(\Re M_{xy})+\frac{\partial}{\partial y}(\Re M_y)-\Re Q_y=\Re m_y\\
&\frac{\partial}{\partial x}(\Re Q_x)+\frac{\partial}{\partial y}(\Re Q_y)+\Re q=-\Re\bar{q}
\end{aligned} \tag{26}$$

Equations (21) and (22) are inserted into equation (26), ones get

$$\begin{aligned}
&-\frac{\partial}{\partial x}\left[D\frac{\partial^2 w_b}{\partial x^2}+D_1\frac{\partial^2 w_b}{\partial y^2}\right]-\frac{\partial}{\partial y}\left[(D-D_1)\frac{\partial^2 w_b}{\partial x\partial y}\right]\\
&\quad -S\frac{\partial w_s}{\partial x}=-\Re\left(J_0\frac{\partial^3 w_b}{\partial x\partial t^2}\right)\\
&-\frac{\partial}{\partial x}\left[(D-D_1)\frac{\partial^2 w_b}{\partial x\partial y}\right]-\frac{\partial}{\partial y}\left[D\frac{\partial^2 w_b}{\partial y^2}+D_1\frac{\partial^2 w_b}{\partial x^2}\right]\\
&\quad -S\frac{\partial w_s}{\partial y}=-\Re\left(J_0\frac{\partial^3 w_b}{\partial y\partial t^2}\right)\\
&S\frac{\partial^2 w_s}{\partial x^2}+S\frac{\partial^2 w_s}{\partial y^2}+\Re q=\Re\left(m_0\frac{\partial^2 w}{\partial t^2}\right)
\end{aligned} \tag{27}$$

First two equations of equation (27) can be rewritten as

$$\begin{aligned}
&\frac{\partial w_s}{\partial x}=-\frac{D}{S}\frac{\partial}{\partial x}\left(\frac{\partial^2 w_b}{\partial x^2}+\frac{\partial^2 w_b}{\partial y^2}\right)+\Re\left(\frac{J_0}{S}\frac{\partial^3 w_b}{\partial x\partial t^2}\right)\\
&\frac{\partial w_s}{\partial y}=-\frac{D}{S}\frac{\partial}{\partial y}\left(\frac{\partial^2 w_b}{\partial x^2}+\frac{\partial^2 w_b}{\partial y^2}\right)+\Re\left(\frac{J_0}{S}\frac{\partial^3 w_b}{\partial y\partial t^2}\right)
\end{aligned} \tag{28}$$

Or

$$\begin{aligned}
w_s&=-\frac{D}{S}\left(\frac{\partial^2 w_b}{\partial x^2}+\frac{\partial^2 w_b}{\partial y^2}\right)+\Re\left(\frac{J_0}{S}\frac{\partial^2 w_b}{\partial t^2}\right)\\
&=\chi(\nabla^2 w_b)+\Re\left(\frac{J_0}{S}\frac{\partial^2 w_b}{\partial t^2}\right)
\end{aligned} \tag{29}$$

Where $\chi=-\frac{D}{S}$.

By introducing equation (29) into equation (11), the displacement formulas in terms of bending component w_b are

$$\begin{aligned}
u&=-z\frac{\partial w_b}{\partial x}+f(z)\frac{\partial}{\partial x}\left[\chi(\nabla^2 w_b)+\Re\left(\frac{J_0}{S}\frac{\partial^2 w_b}{\partial t^2}\right)\right]\\
v&=-z\frac{\partial w_b}{\partial y}+f(z)\frac{\partial}{\partial y}\left[\chi(\nabla^2 w_b)+\Re\left(\frac{J_0}{S}\frac{\partial^2 w_b}{\partial t^2}\right)\right]\\
w&=w_b+\chi(\nabla^2 w_b)+\Re\left(\frac{J_0}{S}\frac{\partial^2 w_b}{\partial t^2}\right)
\end{aligned} \tag{30}$$

It is obvious that the novel theory consists of only one unknown variable-the bending component w_b in its displacement formulas. Another important thing is that the varying of the material properties is considered when establishing the displacement formulas of the proposed theory, this is a significantly different point of this theory in comparison with Shimpi's theory; therefore, Shimpi's theory cannot be applied to analyze heterogeneous plates such as FGM plates. On the contrary, the proposed theory can be employed to analyze both homogeneous and heterogeneous plates.

By introducing equation (30) into equations (21) and (22), ones get

$$\begin{aligned}
\Re M_x&=-D\frac{\partial^2 w_b}{\partial x^2}-D_1\frac{\partial^2 w_b}{\partial y^2}\\
\Re M_y&=-D\frac{\partial^2 w_b}{\partial y^2}-D_1\frac{\partial^2 w_b}{\partial x^2}\\
\Re M_{xy}&=-D\frac{\partial^2 w_b}{\partial x\partial y}+D_1\frac{\partial^2 w_b}{\partial x\partial y}
\end{aligned} \tag{31}$$

$$\begin{aligned}
\Re Q_x&=S\frac{\partial}{\partial x}\left[\chi(\nabla^2 w_b)\right]+\Re\left(J_0\frac{\partial^3 w_b}{\partial x\partial t^2}\right)\\
\Re Q_y&=S\frac{\partial}{\partial y}\left[\chi(\nabla^2 w_b)\right]+\Re\left(J_0\frac{\partial^3 w_b}{\partial y\partial t^2}\right)
\end{aligned} \tag{32}$$

Governing equation

Introducing equations (31) and (32) into equation (26), the governing differential equation of the FGM nanoplate can be written as

$$\begin{aligned}
&S\frac{\partial^2}{\partial x^2}\left[\chi(\nabla^2 w_b)\right]+S\frac{\partial^2}{\partial y^2}\left[\chi(\nabla^2 w_b)\right]\\
&\quad+\Re\left(J_0\frac{\partial^4 w_b}{\partial x^2\partial t^2}+J_0\frac{\partial^4 w_b}{\partial y^2\partial t^2}\right)+\Re q=-\Re\bar{q}
\end{aligned} \tag{33}$$

After some variations, the governing differential equation of the FGM nanoplate is

$$\begin{aligned}
&D(\nabla^2\nabla^2 w_b)-(J_0-\chi m_0)\frac{\partial^2}{\partial t^2}(\nabla^2\Re w_b)\\
&\quad+m_0\frac{\partial^2\Re w_b}{\partial t^2}+\frac{J_0 m_0}{S}\frac{\partial^4\Re\Re w_b}{\partial t^4}+\Re q=0
\end{aligned} \tag{34}$$

This is a simple governing differential equation of the FGM nanoplates, because it consists of only one unknown variable of bending component w_b.

Analytical solutions

In the current work, the Navier procedure is applied to analyze the fully simple supported rectangular

FGM nanoplates. The solution of the plate is assumed as the following formula

$$w_b(x,y)=\sum_{r=1}^{\infty}\sum_{s=1}^{\infty}W_{brs}\sin\varphi x\sin\psi y\sin\omega_{rs}t \tag{35}$$

where $\varphi=r\pi/a$, $\psi=s\pi/b$ and W_{brs} is the quantity to be determined and ω_{rs} is the frequency of free vibration of the FGM nanoplates.

In the case of static bending analysis, by introducing equation (35) into equation (34) without the time items, ones can get the following formula

$$W_{rs}=\frac{Q_{rs}\left(1+\kappa^2\varphi^2+\kappa^2\psi^2\right)}{D\left(\varphi^2+\psi^2\right)^2} \tag{36}$$

where $Q_{rs}=q_0$ for sinusoidal distributed load.

In the case of free vibration analysis, by introducing equation (35) into equation (34), ones can get the biquadratic frequency equation as the following formula

$$\begin{aligned}&\left[1+\kappa\left(\varphi^2+\psi^2\right)\right]^2J_0m_0\omega_{rs}^4\\&\quad-\left[1+\kappa\left(\varphi^2+\psi^2\right)\right]\left[\left(J_0\varphi^2+J_0\psi^2+m_0\right)S\right.\\&\quad\left.+\alpha m_0\left(\varphi^2+\psi^2\right)\right]\omega_{rs}^2+DS\left(\varphi^2+\psi^2\right)^2=0\end{aligned} \tag{37}$$

By solving this biquadratic equation, four roots are archived, the lower positive root is related to the bending mode and the higher positive root is related to the shear mode.

Verified study

In this section, some demonstrative examples are given to validate the accuracy of the proposed theory. The materials properties of FGM nanoplate are given by Sobhy[72] as follows

Ceramic Al_2O_3: $E_c=380\,\text{GPa}$, $\nu_c=0.3$, $\rho_c=3800\,\text{kg/m}^3$;
Metal Al: $E_m=70\,\text{GPa}$, $\nu_m=0.3$, $\rho_m=2707\,\text{kg/m}^3$.

The material properties vary continuously in the thickness direction by

$$E(z)=E_m\left(\frac{E_c}{E_m}\right)^{V_c},\quad \rho(z)=\rho_m\left(\frac{\rho_c}{\rho_m}\right)^{V_c},\quad V_c=\left(\frac{z}{h}+\frac{1}{2}\right)^p \tag{38}$$

Firstly, the present non-dimensional deflections and stresses of square FGM nanoplates with $a=b=10$ subjected to sinusoidal load $q=q_0\sin(x\pi/a)\sin(y\pi/b)$ are compared with those of Sobhy[72] as shown in Table 1. It is noticed that the results of Sobhy[72] are achieved using HSDT. The non-dimensional quantities are calculated by $\bar{w}=w(a/2,b/2).10^2E_ch^3/q_0a^4$, $\bar{\sigma}_x=\sigma_x(a/2,b/2,0).10h/q_0a$, $\bar{\tau}_{xz}=\tau_{xz}(0,b/2,h/2).10h/q_0a$, $\bar{\tau}_{xy}=\tau_{xy}(0,0,-h/2).10h/q_0a$. According to this comparison, the present results are very similar to those of Sobhy[72] for all cases of nonlocal coefficient and materials parameters.

Secondly, the non-dimensional frequency of FGM nanoplates is compared with those introduced by Sobhy[72] as shown in Table 2. It is noticed that the numerical results of Sobhy are achieved using HSDT. For all cases of the nonlocal coefficient κ and aspect ratio a/b, the present results are identical to those of Sobhy.[72]

Thirdly, the non-dimensional fundamental frequency of rectangular isotropic homogeneous nanoplates is compared with those calculated by Zenkour.[61] The comparison is presented in Table 3

Table 1. The comparison of non-dimensional deflection and stresses of square FGM nanoplates ($a/h=10$).

			p				
$(\bar{w},\bar{\sigma}_i)$	κ	Refs	0	0.5	2.5	5.5	10.5
$\bar{w}$	0	Sobhy[72]	2.9603	5.4971	8.8382	10.0219	11.1361
		Present	2.9607	5.4816	8.7638	9.9541	11.1188
	2	Sobhy[72]	5.2977	9.8374	15.8166	17.9350	19.9288
		Present	5.2983	9.8096	15.6835	17.8135	19.8978
$\bar{\sigma}_x(h/2)$	0	Sobhy[72]	19.9550	29.6544	41.8345	50.4378	61.1311
		Present	19.9433	29.3487	41.1517	49.6932	60.5363
	2	Sobhy[72]	35.7108	53.0686	74.8658	90.2620	109.3982
		Present	35.6900	52.5215	73.6437	88.9294	108.3339
$\bar{\tau}_{xz}(0)$	0	Sobhy[72]	2.4618	2.4559	2.1227	2.1679	2.3001
		Present	2.3873	2.2354	1.7194	1.8326	2.1010
	2	Sobhy[72]	4.4056	4.3950	3.7988	3.8796	4.1162
		Present	4.2723	4.0003	3.0771	3.2796	3.7599
$\bar{\tau}_{xy}(-h/2)$	0	Sobhy[72]	10.7450	4.4493	7.5813	8.1777	8.5915
		Present	10.7387	4.4899	7.7104977	8.3180	8.7060
	2	Sobhy[72]	19.2289	7.9624	13.5671	14.6345	15.3751
		Present	19.2177	8.0350	13.79846	14.8856	15.5800

with different values of aspect ratio and side-to-thickness ratio. The non-dimensional frequency is computed by $\bar{\omega} = \omega h\sqrt{\rho/G}$. It can obvious that the present numerical results are in good agreement with those of Zenkour.[61]

Overall, it can conclude that the present theory is compatible to analyze FGM nanoplates with good accuracy and convergence rate.

Numerical results

In this section, a rectangular FGM nanoplate ($a = 10$) is considered to demonstrate the effects of some parameters on the static bending and free vibration behavior. The material properties of two gradients of nanoplates are

Ceramic Al_2O_3: $E_c = 380\,\text{GPa}$, $\nu_c = 0.3$, $\rho_c = 3800\,\text{kg/m}^3$;
Metal Al: $E_m = 70\,\text{GPa}$, $\nu_m = 0.3$, $\rho_m = 2707\,\text{kg/m}^3$.

The following non-dimensional parameters are utilized

$$w^* = w\left(\frac{a}{2},\frac{b}{2}\right)\frac{100E_ch^3}{q_0a^4}, \quad \omega^* = \omega\frac{a^2}{\pi^2}\sqrt{\frac{E_c.h^3}{12(1-\nu^2)}},$$
$$\sigma_x^* = \frac{h}{q_0a}\sigma_x\left(\frac{a}{2},\frac{b}{2}\right), \quad \sigma_y^* = \frac{h}{q_0a}\sigma_y\left(\frac{a}{2},\frac{b}{2}\right),$$
$$\tau_{xy}^* = \frac{h}{q_0a}\tau_{xy}(0,0), \quad \tau_{xz}^* = \frac{h}{q_0a}\tau_{xz}\left(0,\frac{b}{2}\right) \tag{39}$$

Table 2. The comparison of non-dimensional fundamental frequencies of square FGM nanoplates ($a/h = 10$).

		p				
κ	Refs	0	0.5	2.5	5.5	10.5
0	Sobhy[72]	1.9318	1.4969	1.2572	1.2087	1.1609
	Present	1.9317	1.4989	1.2623	1.2126	1.1618
2	Sobhy[72]	1.4441	1.1189	0.9397	0.9035	0.8678
	Present	1.4440	1.1205	0.9436	0.9065	0.8685

Table 4. The non-dimensional deflection of square FGM nanoplates.

		p				
a/h	κ	0	0.5	1	4	10
4	0.0	3.7905	5.6097	7.1689	11.0892	13.5096
	0.5	3.9775	5.8866	7.5227	11.6364	14.1762
	1.0	4.5387	6.7171	8.5840	13.2781	16.1762
	1.5	5.4740	8.1012	10.3528	16.0142	19.5096
	2.0	6.7833	10.0390	12.8292	19.8448	24.1763
10	0.0	2.9607	4.5292	5.8701	8.7307	10.0194
	0.5	3.1068	4.7527	6.1598	9.1615	10.5139
	1.0	3.5451	5.4233	7.0289	10.4540	11.9972
	1.5	4.2756	6.5408	8.4773	12.6082	14.4694
	2.0	5.2983	8.1054	10.5050	15.6241	17.9304
100	0.0	2.8042	4.3255	5.6252	8.2859	9.3613
	0.5	2.9426	4.5389	5.9028	8.6948	9.8232
	1.0	3.3577	5.1793	6.7356	9.9215	11.2091
	1.5	4.0496	6.2466	8.1236	11.9660	13.5189
	2.0	5.0183	7.7407	10.0668	14.8282	16.7527

Table 5. The non-dimensional deflection of rectangular FGM nanoplates ($b/a = 2$).

		p				
a/h	κ	0	0.5	1	4	10
4	0.0	8.7553	13.1261	16.8681	25.6928	30.5958
	0.5	9.0253	13.5309	17.3884	26.4853	31.5394
	1.0	9.8354	14.7454	18.9491	28.8626	34.3704
	1.5	11.1856	16.7696	21.5504	32.8247	39.0886
	2.0	13.0759	19.6035	25.1922	38.3718	45.6942
10	0.0	7.4276	11.3972	14.7901	21.9192	25.0115
	0.5	7.6567	11.7488	15.2463	22.5953	25.7829
	1.0	8.3439	12.8033	16.6148	24.6234	28.0972
	1.5	9.4894	14.5609	18.8956	28.0036	31.9543
	2.0	11.0930	17.0215	22.0887	32.7359	37.3542
100	0.0	7.1772	11.0712	14.3982	21.2076	23.9585
	0.5	7.3986	11.4127	14.8423	21.8617	24.6974
	1.0	8.0627	12.4371	16.1746	23.8240	26.9143
	1.5	9.1695	14.1444	18.3949	27.0945	30.6090
	2.0	10.7190	16.5347	21.5035	31.6732	35.7815

Table 3. The comparison of non-dimensional fundamental frequencies of rectangular homogeneous nanoplates.

			κ^2					
a/h	b/a	Refs	0	1	2	3	4	5
10	1	Zenkour[61]	0.093028	0.085015	0.078769	0.073725	0.069540	0.065996
		Present	0.093028	0.085015	0.078769	0.073725	0.069540	0.065996
	2	Zenkour[61]	0.058883	0.055556	0.052735	0.050305	0.048182	0.046308
		Present	0.058883	0.055556	0.052735	0.050305	0.048182	0.046308
20	1	Zenkour[61]	0.023864	0.021808	0.020206	0.018912	0.017839	0.016929
		Present	0.023864	0.021808	0.020206	0.018912	0.017839	0.016929
	2	Zenkour[61]	0.014965	0.014119	0.013402	0.012785	0.012245	0.011769
		Present	0.014965	0.014119	0.013402	0.012785	0.012245	0.011769

Static bending analysis

Firstly, the numerical investigation of deflection w of rectangular FGM nanoplates subjected to sinusoidal load is presented in this subsection. The non-dimensional deflections w^* of square FGM nanoplates with the variation of the nonlocal coefficient from $\kappa = 0$ to $\kappa = 2$ are shown in Table 4, while the

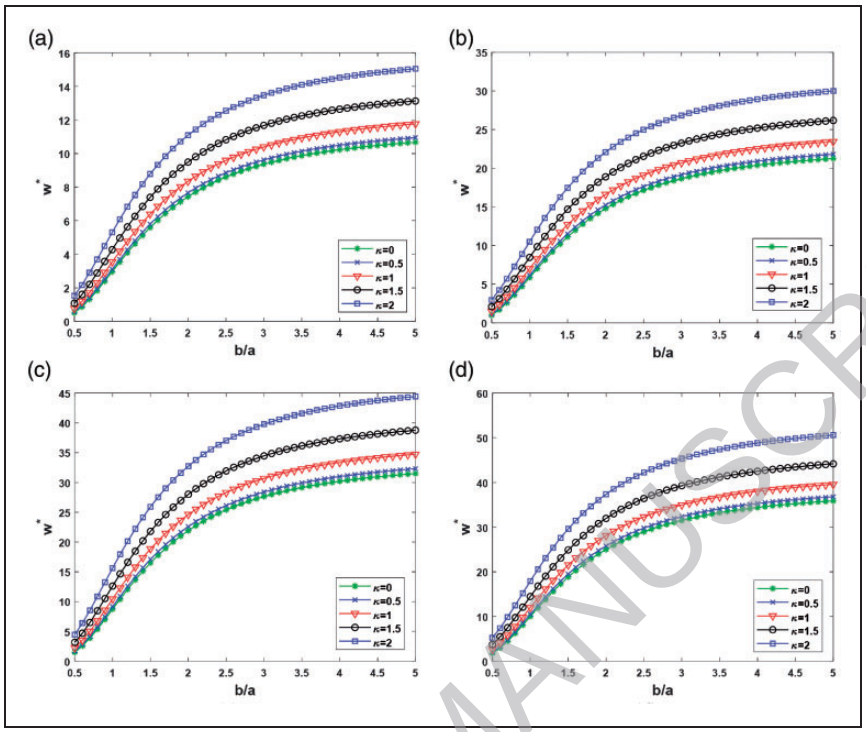

Figure 2. Non-dimensional deflection of FGM nanoplates, (a) $p = 0$, $a/h = 10$, (b) $p = 1$, $a/h = 10$, (c) $p = 4$, $a/h = 10$ and (d) $p = 10$, $a/h = 10$.

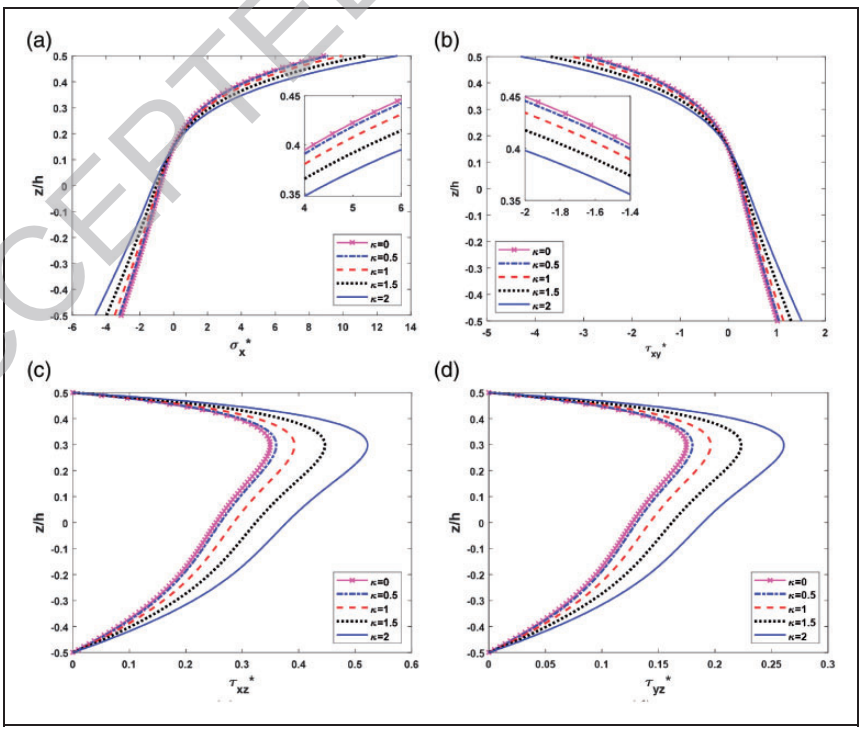

Figure 3. The distribution of stresses through the plate thickness with $p = 5$, $a/h = 10$, $b/a = 2$, (a) normal stress, (b) in-plane shear stress, (c) and (d) transverse shear stresses.

Table 6. The non-dimensional fundamental frequencies of square FGM nanoplates.

		p				
a/h	κ	0	0.5	1	4	10
4	0.0	1.4116	1.2170	1.1029	0.9337	0.8693
	0.5	1.3467	1.1610	1.0522	0.8908	0.8294
	1.0	1.2900	1.1121	1.0079	0.8533	0.7945
	1.5	1.2400	1.0689	0.9688	0.8202	0.7636
	2.0	1.1953	1.0304	0.9339	0.7906	0.7361
10	0.0	1.6304	1.3860	1.2504	1.0801	1.0303
	0.5	1.5554	1.3222	1.1929	1.0304	0.9829
	1.0	1.4899	1.2666	1.1427	0.98706	0.9415
	1.5	1.4321	1.2174	1.0983	0.94873	0.9050
	2.0	1.3805	1.1735	1.0587	0.91455	0.8724
100	0.0	1.6874	1.4289	1.2876	1.1188	1.0747
	0.5	1.6099	1.3632	1.2284	1.0673	1.0253
	1.0	1.5421	1.3058	1.1767	1.0224	0.9821
	1.5	1.4822	1.2551	1.1310	0.9827	0.9440
	2.0	1.4288	1.2099	1.0902	0.9473	0.9099

Table 7. The non-dimensional fundamental frequencies of rectangular FGM nanoplates ($b/a = 2$).

		p				
a/h	κ	0	0.5	1	4	10
4	0.0	0.9349	0.8018	0.7254	0.6186	0.5811
	0.5	0.9074	0.7781	0.7040	0.6004	0.5640
	1.0	0.8821	0.7565	0.6844	0.5837	0.5483
	1.5	0.8588	0.7365	0.6663	0.5683	0.5338
	2.0	0.8373	0.7181	0.6496	0.5540	0.5204
10	0.0	1.0320	0.8760	0.7900	0.6838	0.6539
	0.5	1.0015	0.8502	0.7667	0.6637	0.6347
	1.0	0.9736	0.8265	0.7454	0.6452	0.6170
	1.5	0.9480	0.8047	0.7257	0.6282	0.6007
	2.0	0.9242	0.7846	0.7075	0.6124	0.5857
100	0.0	1.0548	0.8932	0.8048	0.6993	0.6718
	0.5	1.0240	0.8668	0.7811	0.6787	0.6520
	1.0	0.9952	0.8427	0.7594	0.6598	0.6338
	1.5	0.9689	0.8205	0.7393	0.6424	0.6171
	2.0	0.9447	0.7999	0.7208	0.6263	0.6016

results of rectangular FGM nanoplates are presented in Table 5. It can see clearly that increasing the nonlocal coefficient leads to increasing of the deflection, this due to the nonlocal plates are softer than local ones. Also, when the coefficient p increases, the non-dimensional deflection of the plates increases rapidly. The reason of this phenomena is that the small value of p denotes the ceramic-rich plates while the greater value of p denotes the meta-rich ones. On the other hand, Figure 2 shows the dependence of non-dimensional deflections w^* on the change of aspect ratio. It is noticed that the rectangular plates are softer than square ones if other parameters are similar. Figure 3 exposes the variation of the stresses through the plate thickness. The normal stresses σ_x^*, σ_y^* and the in-plane shear stress τ_{xy}^* are nonlinear distribution through the plate thickness, the maximum values of the normal stresses and the in-plane shear stress occur at the top surface. On the other hand, the shear stresses are not parabolic for FGM plates, the maximum values do not occur at the mid-surface of the plates because the neutral surface does not locate at the mid-surface of FGM plate. Furthermore, the stresses of the FGM plate increase when κ increases, it can conclude that the nonlocal plates are softer than local ones.

Free vibration analysis

Secondly, the investigation of free vibration of rectangular FGM nanoplates is exhibited in Tables 6 and 7 and Figures 4 to 7. It can see clearly that the non-dimensional fundamental frequencies of the rectangular FGM nanoplates decrease when increasing the nonlocal coefficient κ for both cases of the square plates and rectangular plates as in Tables 6 and 7. Also, when p increases, the non-dimensional fundamental frequencies of FGM nanoplates decrease. The reason is that when the material parameter increases, the plates become metal-rich plates which are softer than ceramic-rich ones.

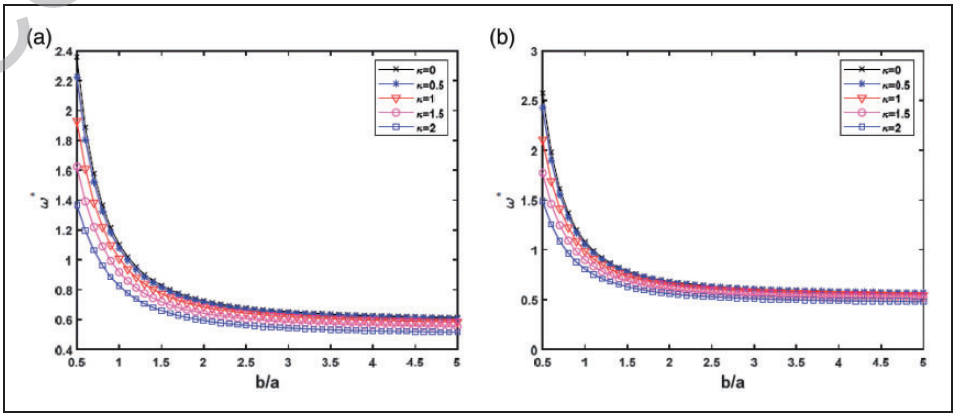

Figure 4. The effects of aspect ratio on the non-dimensional fundamental frequencies of the plates: (a) $p = 1$, $a/h = 4$, (b) $p = 4$, $a/h = 10$.

Furthermore, the graphical investigation of the influences of some parameters on the free vibration behavior of FGM nanoplates are exhibited in Figures 4 to 7. Figure 4 presents the dependence of frequencies of FGM nanoplates on b/a ratio, the FGM nanoplates have intermediate behavior with the change of aspect ratio. As increasing b/a ratio, the non-dimensional frequencies of the plate decrease rapidly. On the contrary, when a/h ratio increases, the non-dimensional frequencies increase for all cases of nonlocal and local plates as publicized in Figure 5. The effects of p on the vibration behavior of FGM nanoplates are shown in Figure 6, it is noticed that the non-dimensional frequencies of the plates decrease by increasing the material parameter. To show more details about the influences of κ on the higher-order frequencies of the FGM nanoplates, the first ten-mode shapes of the plates with different values of the nonlocal coefficient are presented in Figure 7. It is obvious that the variation of the

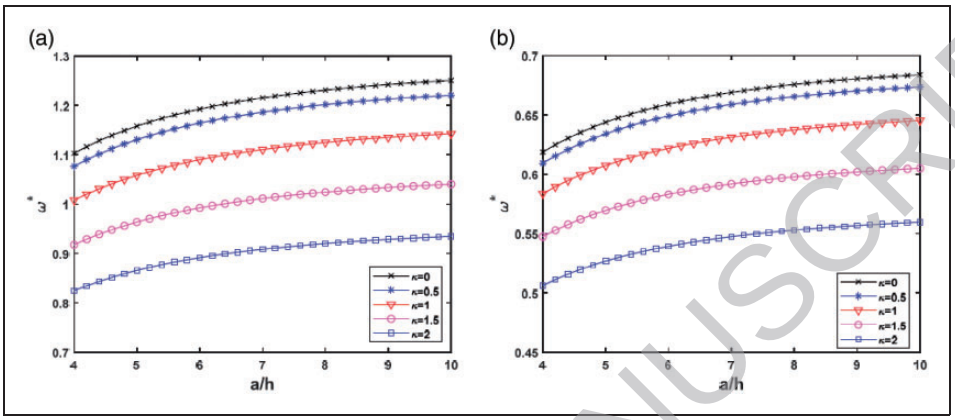

Figure 5. The influences of side-to-thickness ration on the non-dimensional fundamental frequencies of the FGM nanoplates: (a) $p = 1$, $b/a = 1$, (b) $p = 4$, $b/a = 2$.

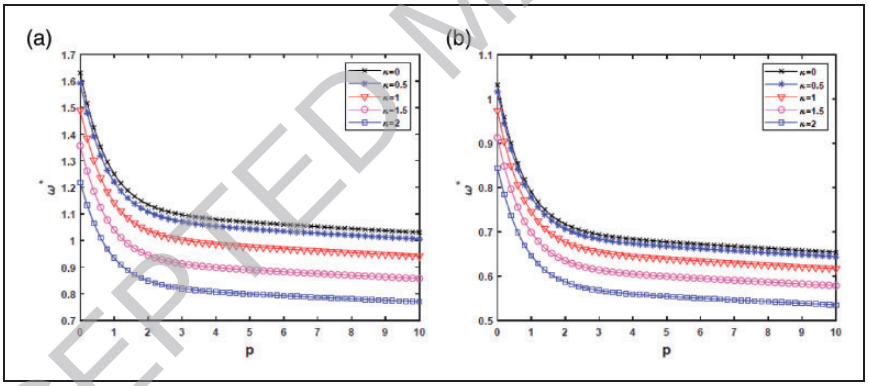

Figure 6. The effects of material parameter on the non-dimensional fundamental frequencies of the FGM nanoplates: (a) $a/h = 10$, $b/a = 1$, (b)$a/h = 10$, $b/a = 2$.

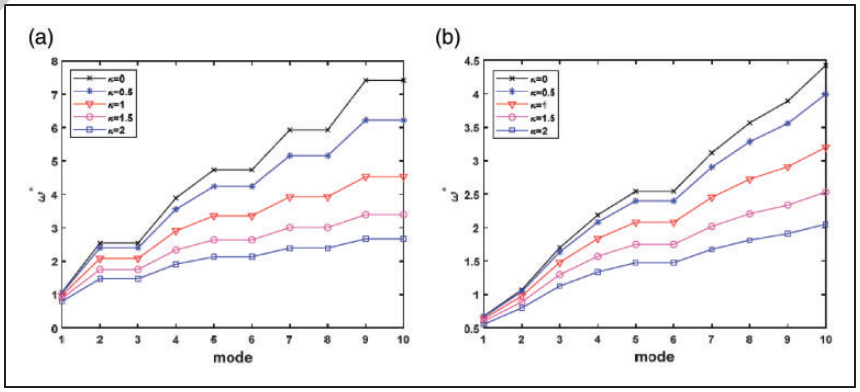

Figure 7. The first ten mode shapes of the FGM nanoplates: (a) $p = 5$, $a/h = 10$, $b/a = 1$, (b)$p = 5$, $a/h = 10$, $b/a = 2$.

nonlocal coefficient has a significant effect on the higher-order frequencies of the FGM nanoplates.

Overall, for all cases of aspect ratios, side-to-thickness ratios or material parameters, the non-dimensional frequencies of the nonlocal FGM nanoplates are smaller than those of local ones, this is an important conclusion of this study.

Conclusions

In conclusion, a novel nonlocal theory based on single variable SDPT has been recognized to evaluate the rectangular FGM nanoplates. Although this theory consists of only one unknown variable in its displacement formulas and its governing differential equations, the shear strains and stresses are quadratic variations and equal to zero at two plate surfaces. This is the most advantage of the proposed theory, because it reduces time and the computation cost to predict behavior of the plates. The governing differential equations have been originated from the equilibrium equation based on NET. The verified study showed that the proposed theory was compatible to analyze FGM nanoplates. A large number of parametric studies have been carried out to study the effects of some parameters on behavior of the FGM nanoplates. These results are useful for further studies and the researcher in similar topics or practical engineering.

Acknowledgements

DVT gratefully acknowledges the support of Vietnam National Foundation for Science and Technology Development (NAFOSTED) under grant number 107.02-2018.30.

Declaration of Conflicting Interests

The author(s) declared no potential conflicts of interest with respect to the research, authorship, and/or publication of this article.

Funding

The author(s) received no financial support for the research, authorship, and/or publication of this article.

ORCID iD

Pham Van Vinh https://orcid.org/0000-0002-8053-6977

References

1. Reddy JN. Analysis of functionally graded plates. *Int J Numer Meth Engng* 2000; 47: 663–684.
2. Javaheri R and Eslami MR. Buckling of functionally graded plates under in-plane compressive loading. *Zeitschrift Für Angewandte Mathematik Und Mechanik* 2002; 82: 277–283.
3. Nam VH, Pham VV, Chinh NV, et al. A new beam model for simulation of the mechanical behaviour of variable thickness functionally graded material beams based on modified first order shear deformation theory. *Materials* 2019; 12: 404.
4. Bui TQ, Do TV, Ton LHT, et al. On the high temperature mechanical behaviors analysis of heated functionally graded plates using FEM and a new third-order shear deformation plate theory. *Compos Part B Eng* 2016; 92: 218–241.
5. Nguyen HN, Hong TT, Vinh PV, et al. An efficient beam element based on quasi-3D theory for static bending analysis of functionally graded beams. *Materials* 2019; 12: 2198.
6. Liessa AW. The free vibration of rectangular plates. *J Sound Vibr* 1973; 31: 257–293.
7. Mohammadi M, Said AR and Jomehzadeh E. Levy solution for buckling analysis of functionally graded rectangular plates. *Appl Compos Mater* 2010; 17: 81–93.
8. Mindlin RD. Influence of rotatory inertia and shear on flexural motions of isotropic, elastic plates. *J Appl Mech* 1951; 18: 31–38.
9. Hosseini-Hashemi S, Taher HRD, Akhavan H, et al. Free vibration of functionally graded rectangular plates using first-order shear deformation plate theory. *Appl Math Modell* 2010; 34: 1276–1291.
10. Hosseini-Hashemi S, Fadaee M and Atashipour SR. A new exact analytical approach for free vibration of Reissner–Mindlin functionally graded rectangular plates. *Int J Mech Sci* 2011; 53: 11–22.
11. Nguyen TK, Sab K and Bonnet G. First-order shear deformation plate models for functionally graded materials. *Compos Struct* 2008; 83: 25–36.
12. Shimpi RP, Patel HG and Arya H. New first-order shear deformation plate theories. *J Appl Mech* 2007; 74: 523–533.
13. Thai HT and Choi DH. A simple first-order shear deformation theory for the bending and free vibration analysis of functionally graded plates. *Compos Struct* 2013; 101: 332–340.
14. Nam VH, Nam NH, Vinh PV, et al. A new efficient modified first-order shear model for static bending and vibration behaviors of two-layer composite plate. *Adv Civil Eng* 2019; 2019: 1–17.
15. Nguyen HN, Hong TT, Vinh PV, et al. A refined simple first-order shear deformation theory for static bending and free vibration analysis of advanced composite plates. *Materials* 2019; 12: 2385.
16. Javaheri R and Eslami MR. Thermal buckling of functionally graded plates based on higher order theory. *J Therm Stress* 2002; 25: 603–625.
17. Ferreira AJM, Batra RC, Roque CMC, et al. Static analysis of functionally graded plates using third-order shear deformation theory and a meshless method. *Compos Struct* 2005; 69: 449–457.
18. Talha M and Singh BN. Static response and free vibration analysis of FGM plates using higher order shear deformation theory. *Appl Math Modell* 2010; 34: 3991–4011.
19. Mantari JL and Guedes Soares C. Finite element formulation of a generalized higher order shear deformation theory for advanced composite plates. *Compos Struct* 2013; 96: 545–553.
20. Mantari JL and Guedes Soares C. Optimized sinusoidal higher order shear deformation theory for the analysis of functionally graded plates and shells. *Compos Part B Eng* 2014; 56: 126–136.

21. Merazi M, Hadji L, Daouadji TH, et al. A new hyperbolic shear deformation plate theory for static analysis of FGM plate based on neutral surface position. *Geomech Eng* 2015; 8: 305–321.
22. Daouadji TH, Tounsi A and Bedia EAA. A new higher order shear deformation model for static behavior of functionally graded plates. *Adv Appl Math Mech* 2013; 5: 351–364.
23. Benferhat R, Hassaine Daouadji T and Said Mansour M. A higher order shear deformation model for bending analysis of functionally graded plates. *Trans Indian Inst Met* 2015; 68: 7–16.
24. Mechab I, Mechab B and Benaissa S. Static and dynamic analysis of functionally graded plates using four-variable refined plate theory by the new function. *Compos Part B Eng* 2013; 45: 748–757.
25. Shimpi RP. Refined plate theory and its variants. *AIAA J* 2002; 40: 137–146.
26. Shimpi RP, Shetty RA and Guha A. A single variable refined theory for free vibrations of a plate using inertia related terms in displacements. *Eur J Mech A/Solid* 2017; 65: 136–148.
27. Zenkour AM. Benchmark trigonometric and 3-D elasticity solutions for an exponentially graded thick rectangular plate. *Arch Appl Mech* 2007; 77: 197–214.
28. Mantari JL and Soares CG. A quasi-3D tangential shear deformation theory with four unknowns for functionally graded plates. *Acta Mech* 2015; 226: 625–642.
29. Mantari JL and Soares CG. Four-unknown quasi-3D shear deformation theory for advanced composite plates. *Compos Struct* 2014; 109: 231–239.
30. Adim B and Daouadji TH. Effects of thickness stretching in FGM plates using a quasi-3D higher order shear deformation theory. *Adv Mater Res* 2016; 5: 223–244.
31. Thai HT and Kim SE. A simple quasi-3D sinusoidal shear deformation theory for functionally graded plates. *Compos Struct* 2013; 99: 172–180.
32. Neves AMA, Ferreira AJM, Carrera E, et al. A quasi-3D hyperbolic shear deformation theory for the static and free vibration analysis of functionally graded plates. *Compos Struct* 2012; 94: 1814–1825.
33. Neves AMA, Ferreira AJM, Carrera E, et al. A quasi-3D sinusoidal shear deformation theory for the static and free vibration analysis of functionally graded plates. *Compos Part B Eng* 2012; 43: 711–725.
34. Carrera E, Brischetto S, Cinefra M, et al. Effects of thickness stretching in functionally graded plates and shells. *Compos Part B Eng* 2011; 42: 123–133.
35. Yang F, Chong ACM, Lam DCC, et al. Couple stress-based strain gradient theory for elasticity. *Int J Solids Struct* 2002; 39: 2731–2743.
36. Gurtin ME, Markenscoff S and Thurston RN. Effect of surface stress on the natural frequency of thin crystals. *Appl Phys Lett* 1976; 29: 529–530.
37. Guo JG and Zhao YP. The size-dependent bending elastic properties of nanobeams with surface effects. *Nanotechnology* 2007; 18: 295701.
38. Wang GF and Feng XQ. Timoshenko beam model for buckling and vibration of nanowires with surface effects. *J Phys D Appl Phys* 2009; 42: 155411.
39. Farshi B, Assadi A and Alinia-Ziazi A. Frequency analysis of nanotubes with consideration of surface effects. *Appl Phys Lett* 2010; 96: 093105.
40. Lu P, He LH, Lee HP, et al. Thin plate theory including surface effects. *Int J Solids Struct* 2006; 43: 4631–4647.
41. Zhou LG and Huang H. Are surface elasticity softer or stiffer. *Appl Phys Lett* 2004; 84: 1940–1942.
42. Fleck N, Muller G, Ashby M, et al. Strain gradient plasticity: theory and experiment. *Acta Metallurgica et Materialia* 1994; 42: 475–487.
43. Aifantis EC and Aifantis EC. Strain gradient interpretation of size effects. *Int J Fract* 1999; 95: 299–314.
44. Sadeghi H, Baghani M and Naghdabadi R. Strain gradient elasticity solution for functionally graded microcylinders. *Int J Eng Sci* 2012; 50: 22–30.
45. Eringen AC. Theory of micropolar plates. *J Appl Math Phys* 1967; 18: 12–30.
46. Eringen AC. Nonlocal polar elastic continua. *Int J Eng Sci* 1972; 10: 1–16.
47. Eringen AC and Edelen DGB. On nonlocal elasticity. *Int J Eng Sci* 1972; 10: 233–248.
48. Eringen AC. On differential equations of nonlocal elasticity and solutions of screw dislocation and surface waves. *J Appl Phys* 1983; 54: 4703–4710.
49. Eringen AC. *Nonlocal continuum field theories*. New York: Springer, 2002.
50. Reddy JN. Nonlocal theories for bending, buckling and vibration of beams. *Int J Eng Sci* 2007; 45: 288–307.
51. Reddy JN and Pang SD. Nonlocal continuum theories of beams for the analysis of carbon nanotubes. *J Appl Phys* 2008; 103: 023511.
52. Zenkour AM. Nonlocal elasticity and shear deformation effects on thermal buckling of a CNT embedded in a viscoelastic medium. *Eur Phys J Plus* 2018; 133: 196.
53. Zenkour AM. A two-unknown nonlocal shear and normal deformations theory for buckling analysis of nanorods. *J Braz Soc Mech Sci Eng* 2020; 42: 358.
54. Ebrahimi F, Barati MR and Zenkour AM. Vibration analysis of smart embedded shear deformable nonhomogeneous piezoelectric nanoscale beams based on nonlocal elasticity theory. *Int J Aeronaut Space Sci* 2017; 18: 255–269.
55. Thai HT and Vo TP. A nonlocal sinusoidal shear deformation beam theory with application to bending, buckling, and vibration of nanobeams. *Int J Eng Sci* 2012; 54: 58–66.
56. Şimşek M and Yurtcu HH. Analytical solutions for bending and buckling of functionally graded nanobeams based on the nonlocal Timoshenko beam theory. *Compos Struct* 2013; 97: 378–386.
57. Eltaher MA, Emam SA and Mahmoud FF. Free vibration analysis of functionally graded size-dependent nanobeams. *Appl Math Comput* 2012; 218: 7406–7420.
58. Nazemnezhad R and Hashemi SH. Nonlocal nonlinear free vibration of functionally graded nanobeams. *Compos Struct* 2014; 110: 192–199.
59. Arefi M, Bidgoli E, Dimitri R, et al. Nonlocal bending analysis of curved nanobeams reinforced by graphene nanoplatelets. *Compos Part B Eng* 2019; 166: 1–12.
60. Sobhy M and Zenkour AM. Nonlocal thermal and mechanical buckling of nonlinear orthotropic viscoelastic nanoplates embedded in a Visco-Pasternak medium. *Int J Appl Mech* 2018; 10: 1850086.
61. Zenkour AM. A novel mixed nonlocal elasticity theory for thermoelastic vibration of nanoplates. *Compos Struct* 2018; 185: 821–833.

62. Zenkour AM and Radwan AF. Nonlocal mixed variational formula for orthotropic nanoplates resting on elastic foundations. *Eur Phys J Plus* 2020; 135: 493.
63. Zenkour AM, Hafed ZS and Radwan AF. Bending analysis of functionally graded nanoscale plates by using nonlocal mixed variational formula. *Mathematics* 2020; 8: 1162.
64. Aghababaei R and Reddy JN. Nonlocal third-order shear deformation plate theory with application to bending and vibration of plates. *J Sound Vibr* 2009; 326: 277–289.
65. Lu BP, Zhang PQ, Lee HP, et al. Non-local elastic plate theories. *Proc R Soc A* 2007; 463: 3225–3240.
66. Aksencer T and Aydogdu M. Levy type solution method for vibration and buckling of nanoplates using nonlocal elasticity theory. *Physica E Low-Dimens Syst Nanostruct* 2011; 43: 954–959.
67. Hashemi SH, Bedroud M and Nazemnezhad R. An exact analytical solution for free vibration of functionally graded circular/annular Mindlin nanoplates via nonlocal elasticity. *Compos Struct* 2013; 103: 108–118.
68. Zenkour AM and Sobhy M. Nonlocal elasticity theory for thermal buckling of nanoplates lying on Winkler-Pasternak elastic substrate medium. *Physica E: Low-Dimens Syst Nanostruct* 2013; 53: 251–259.
69. Alzahrani EO, Zenkour AM and Sobhy M. Small scale effect on hygro-thermo-mechanical bending of nanoplates embedded in an elastic medium. *Compos Struct* 2013; 105: 163–172.
70. Sobhy M. Natural frequency and buckling of orthotropic nanoplates resting on two-parameter elastic foundations with various boundary conditions. *J Mech* 2014; 30: 443–453.
71. Sobhy M. Hygrothermal deformation of orthotropic nanoplates based on the state-space concept. *Compos Part B Eng* 2015; 79: 224–235.
72. Sobhy M. A comprehensive study on FGM nanoplates embedded in an elastic medium. *Compos Struct* 2015; 134: 966–980.
73. Sobhy M and Radwan AF. A new quasi 3D nonlocal plate theory for vibration and buckling of FGM nanoplates. *Int J Appl Mech* 2017; 09: 1750008.
74. Natarajan S, Chakraborty S, Thangavel M, et al. Size-dependent free flexural vibration behavior of functionally graded nanoplates. *Comput Mater Sci* 2012; 65: 74–80.